nature genetics

The noncoding RNA *IPW* regulates the imprinted *DLK1-DIO3* locus in an induced pluripotent stem cell model of Prader-Willi syndrome

Yonatan Stelzer[1], Ido Sagi[1], Ofra Yanuka[1], Rachel Eiges[2] & Nissim Benvenisty[1]

Parental imprinting is a form of epigenetic regulation that results in parent-of-origin differential gene expression. To study Prader-Willi syndrome (PWS), a developmental imprinting disorder, we generated case-derived induced pluripotent stem cells (iPSCs) harboring distinct aberrations in the affected region on chromosome 15. In studying PWS-iPSCs and human parthenogenetic iPSCs, we unexpectedly found substantial upregulation of virtually all maternally expressed genes (MEGs) in the imprinted *DLK1-DIO3* locus on chromosome 14. Subsequently, we determined that *IPW*, a long noncoding RNA in the critical region of the PWS locus, is a regulator of the *DLK1-DIO3* region, as its overexpression in PWS and parthenogenetic iPSCs resulted in downregulation of MEGs in this locus. We further show that gene expression changes in the *DLK1-DIO3* region coincide with chromatin modifications rather than DNA methylation levels. Our results suggest that a subset of PWS phenotypes may arise from dysregulation of an imprinted locus distinct from the PWS region.

Parental imprinting has a crucial role in early embryogenesis and exerts effects later in development, specifically in the placenta and the brain[1]. One of the first human diseases shown to involve parental imprinting was PWS[2]. PWS is a multisystem disorder with an estimated prevalence of approximately 1 in 15,000–25,000 live births[2], resulting from loss of expression of paternally expressed genes (PEGs) that are located on the proximal long arm of chromosome 15 (15q11-q13), often referred to as the PWS region. In most cases (65–75%), loss of expression is caused by microdeletions that include this region. Alternatively, maternal uniparental disomy (mUPD) of chromosome 15 (20–30%) and imprinting defects (1–3%), mostly arising from epimutations, also account for the disease. The PWS region includes a few protein-coding genes and multiple paternally expressed noncoding RNAs, several of which were previously suggested to regulate alternative splicing[3,4]. Nevertheless, the functions of the vast majority of genes residing in the PWS region remain to be determined.

RESULTS

Modeling Prader-Willi syndrome in induced pluripotent stem cells

To model PWS in a human system, we obtained fibroblast cell lines from two PWS cases with distinct aberrations in the PWS region (**Fig. 1a**). We previously reported that regulation of parental imprinting is principally maintained during reprogramming of human somatic cells into iPSCs[5]. PWS fibroblasts were therefore reprogrammed using the four pluripotency factors *POU5F1* (*OCT4*), *SOX2*, *KLF4* and *MYC*[6]. Two weeks after infection of cells with viruses carrying these factors, colonies displaying typical human pluripotent stem cell (PSC)-like morphology appeared in culture. A total of four PWS-iPSC lines were characterized and named PWS-iPSC-1-A, PWS-iPSC-1-B, PWS-iPSC-2-A and PWS-iPSC-2-B. All four iPSC lines exhibited typical morphology, expressed a wide variety of pluripotency markers, had a diploid karyotype (excluding the original chromosomal aberrations) and contributed to all three embryonic germ layers upon differentiation (**Fig. 1b** and **Supplementary Fig. 1a–d**). As expected, comparison of global gene expression in PWS-iPSCs and normal PSCs demonstrated complete downregulation of PEGs in the PWS region (**Fig. 1c**).

Transcriptome analysis in PWS-iPSCs

To study the role of imprinted genes in early human embryogenesis on a genome-wide scale, we recently generated parthenogenetic iPSCs (Pg-iPSCs) that completely lack paternal imprints[7]. Indeed, comprehensive analyses of both gene expression[7] and DNA methylation[8] in Pg-iPSCs uncovered new imprinted genes and imprinted differentially methylated regions (iDMRs) throughout the human genome. Interestingly, gene expression analysis also identified potential targets of imprinted genes[7], suggesting that Pg-iPSCs might serve as a valuable tool for studying complex imprinted disorders. In the current study, we took advantage of the fact that the genome in PWS, lacking a specific subset of paternal alleles, can be considered a special case of the completely maternal parthenogenetic genome. Accordingly, both PWS-iPSCs and Pg-iPSCs exhibited markedly reduced expression levels of PEGs in the PWS region compared with normal PSCs (**Fig. 1d**). Aiming to identify potential targets of PEGs that reside

[1]Stem Cell Unit, Department of Genetics, Institute of Life Sciences, The Hebrew University, Jerusalem, Israel. [2]Stem Cell Research Laboratory, Shaare Zedek Medical Center, The Hebrew University, Jerusalem, Israel. Correspondence should be addressed to N.B. (nissimb@cc.huji.ac.il).

Received 5 December 2013; accepted 3 April 2014; published online 11 May 2014; doi:10.1038/ng.2968

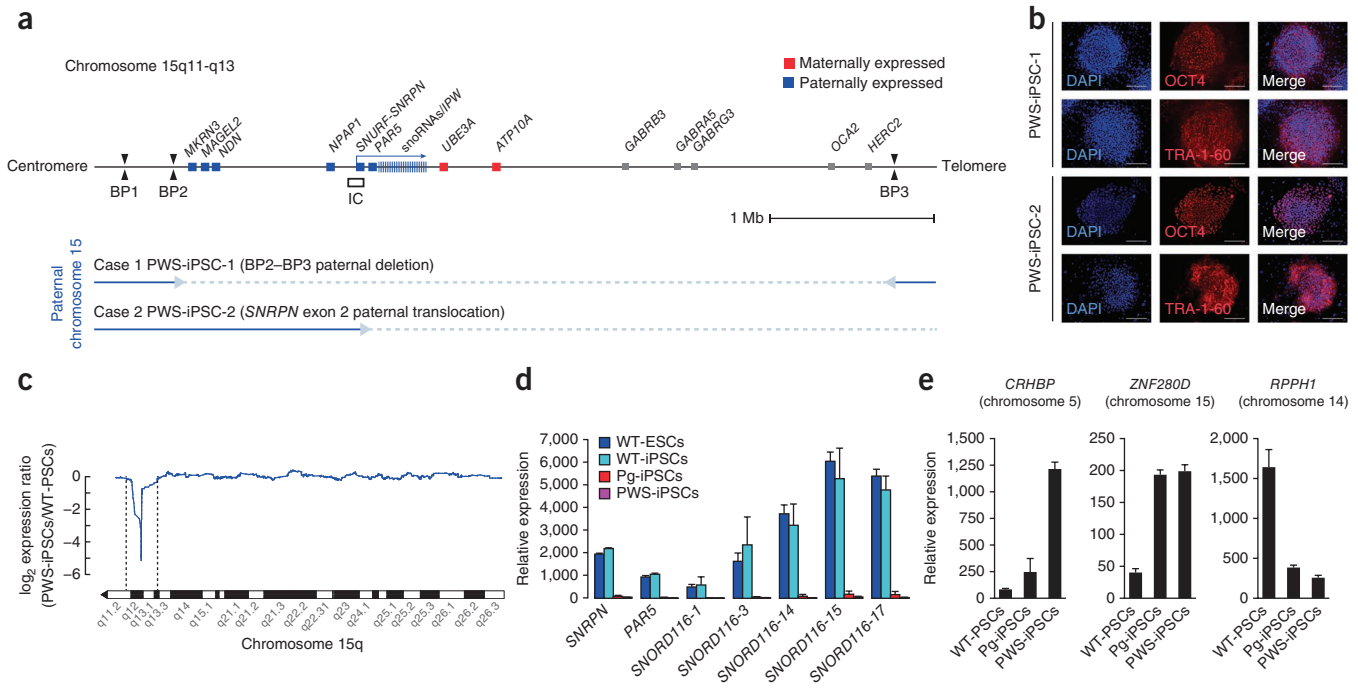

Figure 1 Genome-wide gene expression analysis in PWS-iPSCs. (**a**) Schematic of aberrations in PWS cases with respect to the genomic organization of the PWS region. BP1, BP2 and BP3 represent the most frequent breakpoint sites documented in cases. IC, imprinting control region. (**b**) Immunostaining of undifferentiated PWS-iPSC lines for the OCT4 and TRA-1-60 pluripotency markers. DNA was stained with 4′,6-diamidino-2-phenylindole (DAPI). Scale bars, 200 µm. (**c**–**e**) Genome-wide gene expression analyses were conducted on three PWS-iPSC lines (PWS-iPSC-1-A, PWS-iPSC-1-B and PWS-iPSC-2-A), three Pg-iPSC lines (Pg-iPSC-A-11, Pg-iPSC-A-20 and Pg-iPSC-A-26) and five control PSCs (two iPSC and three ESC lines). WT, wild-type cells. (**c**) Analysis of gene expression by moving average plot along chromosome 15q in PWS-iPSCs relative to normal PSCs (logarithmic scale). Vertical dashed lines mark the genomic region of PWS. (**d**) Mean expression levels ± s.d. of known PEGs in the PWS region. (**e**) Mean expression levels ± s.d. of representative potential targets of PEGs in the PWS locus. Full lists of putative targets can be found in **Supplementary Tables 1** and **2**.

in the PWS region, we needed to set a stringent criterion to minimize the possibility of false positive results. We therefore selected genes that were downregulated by at least 3-fold in both PWS-iPSCs and Pg-iPSCs compared with normal PSCs and identified 43 genes, 32 of which were known PEGs from the PWS region and 11 of which represented potential targets (**Supplementary Table 1**). Alternatively, analyzing genes that were at least 3-fold upregulated resulted in the identification of 12 potential targets (**Supplementary Table 2**). Most of these putative targets did not cluster together in specific genomic regions (**Fig. 1e**), and, although some could not have been detected by comparing mature fibroblasts (for example, *CRHBP*; **Supplementary Fig. 1e**), others showed differential expression between PWS and control parental cells as well (for example, *ZNF280D* and *RPPH1*; **Supplementary Fig. 1e**).

Gene expression in the *DLK1-DIO3* locus is altered in PWS cells

Six of the upregulated genes were known MEGs that reside in the imprinted *DLK1-DIO3* region on chromosome 14 (**Fig. 2a**,**b**). This upregulation of MEGs was unique to PWS-iPSCs and Pg-iPSCs, as it could not be detected in previously reported normal iPSCs nor in model cell lines for diseases, such as iPSCs for fragile-X syndrome[9] (**Fig. 2b**). To further study whether this upregulation involved all known MEGs in the *DLK1-DIO3* region, we complemented the global gene expression analysis by also performing global microRNA (miRNA) expression analysis, which indicated that virtually all MEGs and miRNAs in this locus were upregulated by more than threefold compared with normal PSCs (**Fig. 2c**). To further verify that this upregulation of MEGs in the *DLK1-DIO3* region was associated with PWS, we obtained cells from a third PWS case who, instead of a deletion, harbored mUPD of chromosome 15 (**Supplementary Fig. 2a**). These cells were used to generate and characterize an additional PWS-iPSC line (named PWS-iPSC-3), which exhibited complete downregulation of all PEGs in the PWS region, along with markedly higher levels of MEGs in the *DLK1-DIO3* locus (**Supplementary Fig. 2b**,**c**). As our collection of PWS-iPSCs were derived from unrelated individuals with distinct genetic causes of PWS, our results together suggest that upregulation of MEGs in the *DLK1-DIO3* region is a characteristic of this disease.

As Pg-iPSCs carry two maternal copies of the genome, MEGs are expected to exhibit twofold higher expression in these cells compared with normal PSCs. Therefore, the >3-fold upregulation of all maternal transcripts in the *DLK1-DIO3* region suggested that these genes are coregulated. We previously demonstrated that downregulation of a newly identified PEG in Pg-iPSCs, serving as an antisense regulator, resulted in >3-fold upregulation of its corresponding miRNA targets[10]. *RTL1* is a known PEG in the *DLK1-DIO3* region that is transcribed in antisense orientation to the maternal transcripts in this locus (**Fig. 2a** and **Supplementary Fig. 3a**)[11]. To study whether downregulation of *RTL1* in Pg-iPSCs facilitated upregulation of the *DLK1-DIO3* MEG expression, we specifically knocked down *RTL1* in normal PSCs (**Supplementary Fig. 3b**). Our data showed that downregulation of *RTL1* did not affect the expression of maternal genes in this locus (**Supplementary Fig. 3b**).

The surprising finding that PWS-iPSCs also exhibited elevated expression levels of all maternal transcripts in the *DLK1-DIO3* region, similar to Pg-iPSCs, implied that these genes are potential targets of PEGs from the PWS region. Notably, our previous genome-wide analysis of miRNAs in Pg-iPSCs identified upregulation of both miRNAs

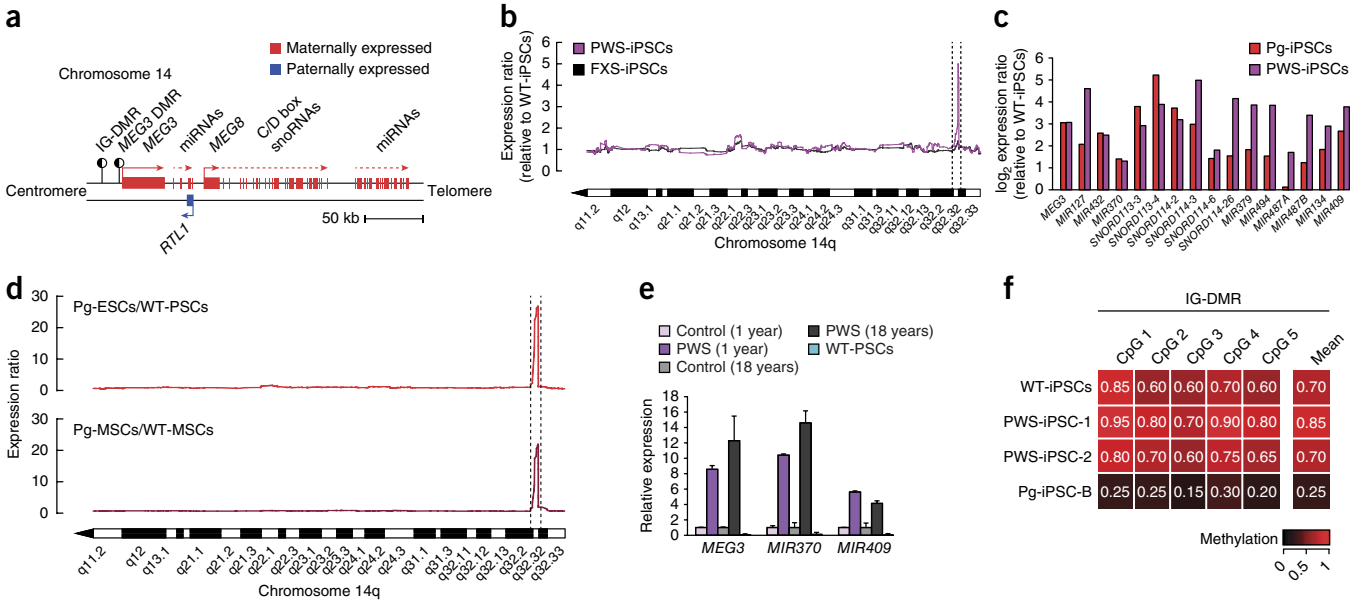

Figure 2 Characterization of the *DLK1-DIO3* locus in PWS. (**a**) Organization of all known MEGs in the *DLK1-DIO3* region. (**b**) Analysis of gene expression by moving average plot along chromosome 14q in 4 PWS-iPSCs and 4 fragile-X syndrome (FXS) iPSCs, relative to 13 normal PSCs (6 iPSC and 7 ESC lines). Vertical dashed lines mark the genomic boundaries of the *DLK1-DIO3* region. (**c**) Gene expression of MEGs in the *DLK1-DIO3* locus, demonstrating upregulation in both Pg-iPSCs (three biological replicates) and PWS-iPSCs (two biological replicates) compared with normal PSCs (two biological replicates; logarithmic scale). (**d**) Analysis of gene expression by moving average plot along chromosome 14q in Pg-ESCs and Pg-MSCs relative to control PSCs and MSCs. Vertical dashed lines mark the genomic boundaries of the *DLK1-DIO3* region. (**e**) qRT-PCR of the mean relative fold change ± s.d. of three technical replicates in *MEG3*, *MIR370* and *MIR409* levels in cerebrum brain tissues derived from two individuals with PWS (1 and 18 years old) and age- and sex-matched control individuals. (**f**) Pyrosequencing analysis of DNA methylation at the IG-DMR of the *DLK1-DIO3* locus. Color is coded from 0 to 1, signifying hypomethylation and hypermethylation, respectively.

that reside in the *DLK1-DIO3* region, as well as of the oncogenic miRNA-371-373 cluster[7,10]. We therefore confirmed that upregulation of MEGs in PWS-iPSCs was restricted to the *DLK1-DIO3* region rather than simply representing general loss of imprinting in these cells (**Supplementary Fig. 3c**,**d**). Furthermore, to rule out the possibility that the higher MEG expression levels resulted from stochastic epigenetic defects acquired during the process of cellular reprogramming of somatic cells to iPSCs, we analyzed expression data from human parthenogenetic embryonic stem cells[12] (Pg-ESCs). Pg-ESCs are derived from the blastocyst after *in vitro* manipulation of human oocytes, thus representing a different source of PSCs. In support of our findings and similar to their Pg-iPSC counterparts, Pg-ESCs also exhibited markedly higher levels of expression of all MEGs in the *DLK1-DIO3* region (**Fig. 2d**).

Next, we asked whether the upregulation of MEGs in PWS-iPSCs was dependent on tissue type. Analysis of expression data from Pg-ESC–derived mesenchymal stem cells (Pg-MSCs) recapitulated the observed effect of MEG upregulation in the *DLK1-DIO3* region (**Fig. 2d**). In addition, we analyzed the expression of *DLK1-DIO3* MEGs in the parental PWS fibroblasts from which the PWS-iPSCs were derived, as well as in B lymphocyte cell lines from two additional PWS cases, which represent a more prevalent source of cells for studying PWS in humans (**Supplementary Fig. 4a**,**b**). We could detect modest differences in the expression of MEGs in the *DLK1-DIO3* region between normal and PWS fibroblasts, yet no expression was found in B lymphocytes (**Supplementary Fig. 4a**,**b**). The relatively moderate effect observed in the parental fibroblasts might be attributable to the intrinsic heterogeneity in primary cell populations. Indeed, close examination of gene-specific effects in the *DLK1-DIO3* region showed that, whereas control undifferentiated cells exhibited relatively low MEG expression levels, control fibroblast cells displayed variable expression levels (**Supplementary Fig. 4c**). These cell type–specific differences might explain the different observations of altered MEG expression in undifferentiated and differentiated cells. As the vast majority of individuals with PWS also display mild to moderate mental retardation, we asked whether this upregulation of MEGs was also evident in mature brain tissue and thus potentially involved in some of the neurological phenotypes. MEGs in the *DLK1-DIO3* region exhibit high expression levels specifically in the frontal cortex. We therefore obtained postmortem cerebrum samples derived from two individuals with PWS (1 and 18 years old), as well as from age- and sex-matched control individuals. Expression levels of representative MEGs, spanning the entire *DLK1-DIO3* region, were markedly higher in PWS brain samples compared with controls (**Fig. 2e**). Notably and similar to the case in mature fibroblasts, the baseline expression levels of MEGs in control brain samples were significantly higher than in control undifferentiated cells and might thus result in overall smaller effects between individuals (**Fig. 2e**). Collectively, our results imply that the upregulation of MEGs in the *DLK1-DIO3* region is evident, although variable in different tissues, with the most profound effect observed in the undifferentiated state.

A possible explanation for the upregulation of MEGs in PWS-iPSCs is that, independent of their aberrations in the PWS region, these cells also carry imprinting abnormalities in the *DLK1-DIO3* region. The paternal germline-derived imprinted DMR (IG-DMR) in the *DLK1-DIO3* region controls the monoallelic expression of genes in this locus[1]. We therefore studied DNA methylation levels at the IG-DMR in both individuals with PWS (**Fig. 2f**). In contrast to Pg-iPSCs, which lack a paternal signature and consequently exhibited hypomethylation of the IG-DMR, PWS-iPSCs showed a differential DNA methylation signature that overall resembled that of normal PSCs (**Fig. 2f**). Moreover, using different heterozygous SNPs in the

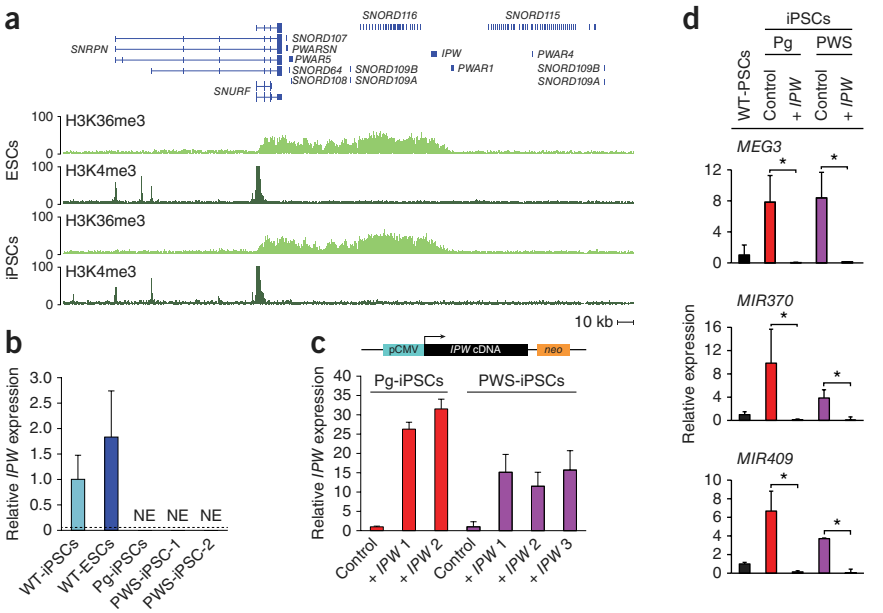

Figure 3 *IPW* regulates gene expression at the *DLK1-DIO3* locus. (**a**) Regional view of the PWS locus demonstrating typical chromatin marks for lncRNAs. Significant enrichment is shown for H3K36me3 and H3K4me3 modifications in two representative PSC cell lines from the ENCODE Project. (**b**) qRT-PCR of the mean relative fold change (± s.d. of two technical replicates) in *IPW* levels in different cell lines. NE, not expressed. (**c**) qRT-PCR of the mean relative fold change (± s.d. of three technical replicates) in *IPW* levels following its overexpression in Pg-iPSCs and PWS-iPSCs. The expression construct is shown above. (**d**) qRT-PCR of the mean relative fold change (± s.d. of three technical replicates) in *MEG3*, *MIR370* and *MIR409* levels in Pg-iPSCs and PWS-iPSCs overexpressing *IPW*. $*P < 1 \times 10^{-5}$, two-tailed unpaired Student's *t* test.

three PWS cases, we demonstrated proper monoallelic expression of both *MEG3* and *RTL1* (**Supplementary Fig. 5**). Taken together, these data demonstrate that upregulation of *DLK1-DIO3* MEGs is restricted to the already expressed maternal allele rather than simply representing improper expression from the paternal allele in PWS-iPSCs. Furthermore, our data suggest that this upregulation is directly associated with downregulation of PEGs in PWS-iPSCs.

IPW regulates expression in the *DLK1-DIO3* locus

Recently, three individuals with overlapping deletions encompassing the minimal region of PWS were reported[13–15]. This minimal region includes a large cluster of paternally expressed small nucleolar RNAs (snoRNAs), shown to form a new class of long noncoding RNAs (lncRNAs)[4], as well as *IPW*, a lncRNA of unknown function[16] (**Fig. 1a**). Indeed, the chromatin signature spanning the minimal PWS region in PSCs showed typical characteristics of transcribed regions and lncRNAs[17], comprising marks of histone 3 lysine 4 trimethylation (H3K4me3) at the *SNURF-SNRPN* transcription start site and histone 3 lysine 36 trimethylation (H3K36me3) along the transcribed region (**Fig. 3a**). LncRNAs were shown to regulate gene expression both in *cis* and in *trans*[18,19] through association with chromatin modifiers[20], thus raising the possibility that one of the transcripts in the minimal PWS region might regulate the expression of MEGs in the *DLK1-DIO3* locus. As the above-mentioned snoRNA cluster was previously linked with post-transcriptional regulation[3,4], we sought to determine whether *IPW* might regulate the expression of the MEGs on chromosome 14. *IPW* was abundantly expressed in normal PSCs and, as with other PEGs in the PWS region, was completely downregulated in Pg-iPSCs and PWS-iPSCs (**Fig. 3b**). We therefore overexpressed *IPW* in both Pg-iPSCs and PWS-iPSCs (**Fig. 3c**) and studied effects on the expression of representative MEGs spanning the entire *DLK1-DIO3* locus (**Fig. 3d**). We found significant downregulation of the expression of these MEGs following introduction of *IPW* in both cell types (**Fig. 3d**). This effect was specific to *IPW* and did not occur following overexpression of the *HOTAIR* lncRNA (**Supplementary Fig. 6a**,**b**), which is known to target the *HOXD* locus in *trans*[19].

IPW affects chromatin in the *DLK1-DIO3* locus

It was previously emphasized that lncRNA-associated gene regulation is mediated by changes in chromatin[19]. We therefore used established chromatin maps in multiple PSC lines (from the Encyclopedia of DNA Elements (ENCODE) Project) in our search for repressive marks in the *DLK1-DIO3* region (**Fig. 4a**). Three enrichment sites, marked by the repressive modifications of histone 3 lysine 27 trimethylation (H3K27me3) and lysine 9 trimethylation (H3K9me3), were identified in the *DLK1* promoter, the IG-DMR and the region upstream of the snoRNA-113 cluster (**Fig. 4a**). We then performed chromatin immunoprecipitation analysis followed by quantitative PCR (ChIP-qPCR) at these three sites. Our results in normal PSCs were consistent with previous findings, demonstrating enrichment of repressive chromatin marks at the *DLK1* promoter, the IG-DMR and the region upstream of the snoRNA-113 cluster (**Fig. 4a**,**b**). In comparing our ChIP-qPCR data across the different cell types, we found significantly lower levels of H3K9me3 marks at the IG-DMR in both Pg-iPSCs and PWS-iPSCs relative to normal PSCs (**Fig. 4b**). This phenotype was fully rescued by the introduction of *IPW* into Pg-iPSCs and PWS-iPSCs (**Fig. 4b**). Next, we asked whether the repressive H3K9me3 mark was regulated in a monoallelic or biallelic manner in normal PSCs. By using an informative SNP in the IG-DMR, we showed that this repressive modification normally exists on both the paternal and maternal alleles (**Supplementary Fig. 6c**). Collectively, our results indicate a direct role for *IPW* in regulating transcriptional repression at the *DLK1-DIO3* locus. Moreover, the effect of *IPW* on chromatin is not prevalent throughout the entire *DLK1-DIO3* locus. Rather, it is restricted to the IG-DMR, which may explain the effect of *IPW* on the expression of all MEGs in this region. Notably, in an orthogonal experiment, knockdown of *IPW* in normal PSCs had no effect on the expression of MEGs in the *DLK1-DIO3* region (data not shown). This result suggests that even low levels of *IPW* are sufficient to maintain chromatin repression at the *DLK1-DIO3* region. Alternatively, it is possible that, whereas *IPW* is required for chromatin repression in early development, its downregulation may be insufficient to remove pre-existing H3K9me3 marks. To further elucidate the mechanism by which *IPW* might regulate the expression of MEGs in the *DLK1-DIO3* region, we studied the potential protein interactions of *IPW*. Among the genes that were significantly downregulated in both Pg-iPSCs and PWS-iPSCs was *ZFP57* (**Supplementary Fig. 6d** and **Supplementary Table 1**), which was described to encode a regulator of imprints within the *DLK1-DIO3* locus[21]. It is therefore possible that *IPW* positively regulates the expression of *ZFP57* in early embryogenesis.

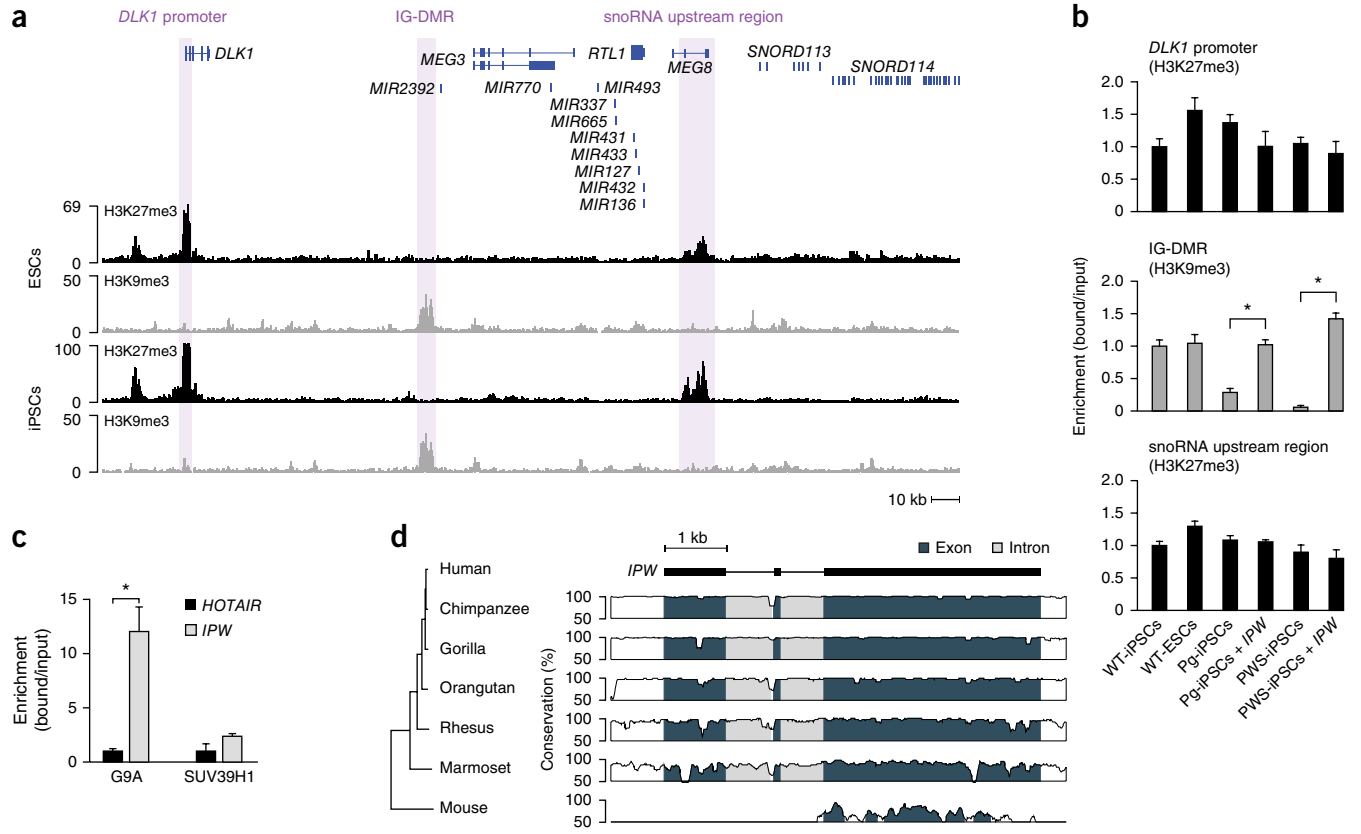

Figure 4 *IPW* affects chromatin modifications at the *DLK1-DIO3* locus. (**a**) Regional view of the *DLK1-DIO3* locus, showing enrichment sites of repressive chromatin marks that were further analyzed using ChIP-qPCR (shaded). (**b**) ChIP-qPCR analysis of the repressive histone marks H3K27me3 and H3K9me3 in Pg-iPSCs and PWS-iPSCs before and after overexpression of *IPW*. Shown is relative enrichment (± s.d. of three technical replicates) at different sites along the *DLK1-DIO3* region. All samples were normalized to input DNA. $*P < 1 \times 10^{-6}$, two-tailed unpaired Student's *t* test. (**c**) RIP was conducted with antibodies against SUV39H1 and G9A and followed by qRT-PCR for the detection of *IPW* transcript. Shown are mean values ± s.d. of two biological replicates. *HOTAIR* served as a negative control. All samples were normalized to input. $*P < 0.0001$, two-tailed unpaired Student's *t* test. (**d**) Conservation analysis of *IPW* among different species, demonstrating low conservation between mice and primates. The *y* axis represents the level of conservation, calculated over 100-bp sliding windows.

However, our results showed that overexpression of *IPW* in both Pg-iPSCs and PWS-iPSCs had no effect on the expression of *ZFP57* (**Supplementary Fig. 6d**). Next, we attempted to identify a possible interaction between *IPW* and histone H3K9 methyltransferases. Both the SUV39H1 and G9A proteins are capable of catalyzing mono-, di- and trimethylation reactions at H3K9 (ref. 22). We therefore performed RNA immunoprecipitation (RIP) in control PSCs followed by quantitative RT-PCR (qRT-PCR) to detect possible enrichment of the *IPW* transcript. As a negative control, we analyzed *HOTAIR*, which was shown to bind to the PRC2 protein complex that catalyzes H3K27 methylation[19]. Our results indicate that *IPW* interacts with G9A (**Fig. 4c**), thus providing strong mechanistic evidence for the function of *IPW* in establishing the H3K9me3 modification at the IG-DMR of the *DLK1-DIO3* locus.

DISCUSSION

The emerging field of disease modeling has been greatly advanced by the generation of iPSCs, which allow modeling of rare disorders and specific disease variations within affected individuals[23,24]. PWS usually arises from *de novo* mutations, thereby limiting the possibility of modeling this disease using ESCs derived after preimplantation genetic diagnosis. Following up on previous reports of successful generation of PWS-iPSCs[25,26], in this study, we established PWS-iPSCs by reprogramming case-derived fibroblasts. Taking advantage of the fact that PWS can be considered to be a special case of completely maternal expression, we compared the gene expression profiles of both PWS-iPSCs and Pg-iPSCs to uncover specific targets of PEGs within the PWS locus on chromosome 15. Notably, we have previously shown high variability in the overall gene expression signature between parthenogenetic and parental, normal fibroblast cell populations[7]. Therefore, to reduce the variability among the different cell types, we conducted our gene expression analysis in the reprogrammed pluripotent state. Surprisingly, our analysis uncovered aberrant expression of all MEGs residing in the *DLK1-DIO3* locus on chromosome 14. This upregulation of MEGs was detected across several tissues and cell types derived from five independent individuals with PWS, including PSCs, fibroblasts and frontal cortex brain tissue. We further show that this phenomenon is mediated by *IPW*, a previously identified imprinted lncRNA[16] of unknown function that originates from the minimal region of PWS[13–15]. LncRNAs are characterized by tissue-specific expression and low conservation across distant species[27]. Indeed, *IPW* is highly conserved among primates but shows little conservation between humans and mice (**Fig. 4d**), indicating functional divergence during the evolution of imprinting regulation. Furthermore, we have recently shown that many iDMRs are not conserved between humans and mice, including human-specific iDMRs that reside in the PWS region[8]. Taken together, these results may explain why mouse models of PWS fail to recapitulate many of the phenotypes associated with this disease in humans[28].

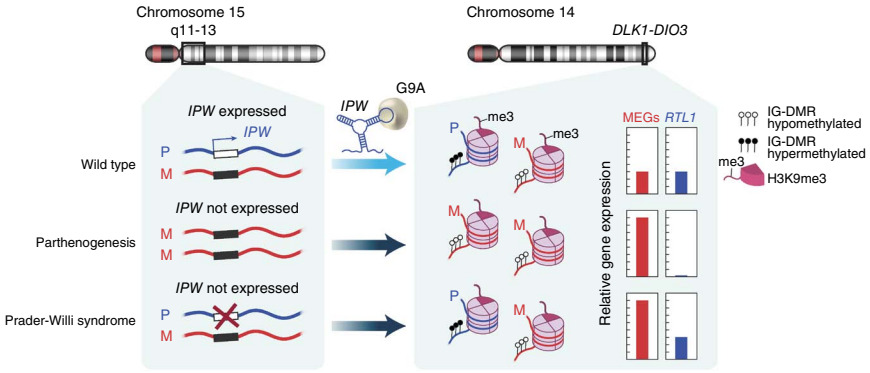

Figure 5 Model summarizing the effect of *IPW* depletion on the expression of MEGs in the *DLK1-DIO3* region during early development. *IPW* is normally expressed from the paternal (P) and not the maternal (M) allele and regulates H3K9me3 modification at the differentially methylated IG-DMR through interaction with the G9A methyltransferase. In parthenogenetic and PWS cells, where *IPW* is absent owing to loss of imprinting, H3K9me3 is not established and the expression of MEGs in the *DLK1-DIO3* region is upregulated. In parthenogenesis, unlike in PWS, the IG-DMR is hypomethylated, leading to downregulation of *RTL1* expression.

In conclusion, we propose a model in which lack of expression of *IPW* in both Pg-iPSCs and PWS-iPSCs results in aberrant upregulation of MEGs in the *DLK1-DIO3* locus (**Fig. 5**). This upregulation is not due to hypermethylation of the IG-DMR in the *DLK1-DIO3* region but rather is caused by depletion of repressive chromatin marks, facilitated by the absence of *IPW* (**Fig. 5**). Our data support the notion that, as was previously implied for other lncRNAs[18], *IPW* interacts with the histone methyltransferase G9A to target the imprinted *DLK1-DIO3* region. Moreover, we demonstrate that the expression of all MEGs in this locus is controlled by the IG-DMR and that changes at the level of histone modification are sufficient to cause significant alterations in their expression. Direct correlation between the expression of specific imprinted genes on chromosome 15 and the complex phenotypes of PWS is only partially understood. Our finding of aberrant expression of MEGs in the *DLK1-DIO3* locus in both the early development of individuals with PWS and in mature brain tissues may shed light on the underlying cause of some of the symptoms observed in PWS. This notion is supported by reports of affected individuals with mUPD of chromosome 14 who display PWS-like phenotypes[29–31], including neonatal hypotonia, small hands and feet, mental retardation and hyperphagia resulting in obesity beyond infancy[29]. Notably, these data suggest that some of the phenotypes of PWS may be caused by aberrant expression of MEGs within the *DLK1-DIO3* region.

Finally, conventional perceptions in the field of parental imprinting support the theory that differentially marked regions throughout the genome provide a selective advantage in the prevention of asexual reproduction in placental mammals. It was also suggested that parent-of-origin expression of certain genes orchestrates what is termed the 'parental conflict theory' (ref. 32). Nevertheless, a functional link between distinct imprinted regions has yet to be reported. Therefore, the cross-talk between the PWS and *DLK1-DIO3* loci in early human development suggests that parental imprinting is a much broader and more complex phenomenon than previously appreciated.

URLs. Coriell Institute for Medical Research, http://www.coriell.org/; National Institute of Child Health and Human Development (NICHD) Brain and Tissue Bank for Developmental Disorders, http://medschool.umaryland.edu/btbank/.

METHODS

Methods and any associated references are available in the online version of the paper.

Accession codes. Microarray gene expression data have been deposited in the Gene Expression Omnibus (GEO) under accession GSE56136.

Note: Any Supplementary Information and Source Data files are available in the online version of the paper.

ACKNOWLEDGMENTS

Fibroblasts obtained from an individual with PWS harboring complete mUPD of chromosome 15 were kindly donated by V. Gross-Tsur (Multidisciplinary Prader-Willi Syndrome Clinic, Child Neurology Unit, Shaare Zedek Medical Center). This research was partially funded by the Israel Science Foundation–Morasha Foundation (grant 1252/12) and by the Israel Ministry of Science and Technology Infrastructure (grant 3-9693).

AUTHOR CONTRIBUTIONS

Y.S. contributed to the conception and design of the study, the collection and assembly of data, data analysis and interpretation, and manuscript writing. I.S. contributed to the collection and assembly of data and graphic design. O.Y. and R.E. contributed to the collection and assembly of data. N.B. contributed to the conception and design of the study, financial support, data analysis and interpretation, and manuscript writing.

COMPETING FINANCIAL INTERESTS

The authors declare no competing financial interests.

1. Ferguson-Smith, A.C. Genomic imprinting: the emergence of an epigenetic paradigm. *Nat. Rev. Genet.* **12**, 565–575 (2011).
2. Cassidy, S.B., Schwartz, S., Miller, J.L. & Driscoll, D.J. Prader-Willi syndrome. *Genet. Med.* **14**, 10–26 (2012).
3. Kishore, S. & Stamm, S. The snoRNA HBII-52 regulates alternative splicing of the serotonin receptor 2C. *Science* **311**, 230–232 (2006).
4. Yin, Q.F. *et al.* Long noncoding RNAs with snoRNA ends. *Mol. Cell* **48**, 219–230 (2012).
5. Pick, M. *et al.* Clone- and gene-specific aberrations of parental imprinting in human induced pluripotent stem cells. *Stem Cells* **27**, 2686–2690 (2009).
6. Takahashi, K. *et al.* Induction of pluripotent stem cells from adult human fibroblasts by defined factors. *Cell* **131**, 861–872 (2007).
7. Stelzer, Y., Yanuka, O. & Benvenisty, N. Global analysis of parental imprinting in human parthenogenetic induced pluripotent stem cells. *Nat. Struct. Mol. Biol.* **18**, 735–741 (2011).
8. Stelzer, Y. *et al.* Identification of novel imprinted differentially methylated regions by global analysis of human-parthenogenetic-induced pluripotent stem cells. *Stem Cell Reports* **1**, 79–89 (2013).
9. Urbach, A., Bar-Nur, O., Daley, G.Q. & Benvenisty, N. Differential modeling of fragile X syndrome by human embryonic stem cells and induced pluripotent stem cells. *Cell Stem Cell* **6**, 407–411 (2010).
10. Stelzer, Y., Sagi, I. & Benvenisty, N. Involvement of parental imprinting in the antisense regulation of onco-miR-372-373. *Nat. Commun.* **4**, 2724 (2013).
11. Seitz, H. *et al.* Imprinted microRNA genes transcribed antisense to a reciprocally imprinted retrotransposon-like gene. *Nat. Genet.* **34**, 261–262 (2003).
12. Vassena, R. *et al.* Accumulation of instability in serial differentiation and reprogramming of parthenogenetic human cells. *Hum. Mol. Genet.* **21**, 3366–3373 (2012).
13. de Smith, A.J. *et al.* A deletion of the HBII-85 class of small nucleolar RNAs (snoRNAs) is associated with hyperphagia, obesity and hypogonadism. *Hum. Mol. Genet.* **18**, 3257–3265 (2009).
14. Duker, A.L. *et al.* Paternally inherited microdeletion at 15q11.2 confirms a significant role for the SNORD116 C/D box snoRNA cluster in Prader-Willi syndrome. *Eur. J. Hum. Genet.* **18**, 1196–1201 (2010).

15. Sahoo, T. *et al.* Prader-Willi phenotype caused by paternal deficiency for the HBII-85 C/D box small nucleolar RNA cluster. *Nat. Genet.* **40**, 719–721 (2008).
16. Wevrick, R., Kerns, J.A. & Francke, U. Identification of a novel paternally expressed gene in the Prader-Willi syndrome region. *Hum. Mol. Genet.* **3**, 1877–1882 (1994).
17. Guttman, M. *et al.* Chromatin signature reveals over a thousand highly conserved large non-coding RNAs in mammals. *Nature* **458**, 223–227 (2009).
18. Guttman, M. *et al.* lincRNAs act in the circuitry controlling pluripotency and differentiation. *Nature* **477**, 295–300 (2011).
19. Rinn, J.L. *et al.* Functional demarcation of active and silent chromatin domains in human *HOX* loci by noncoding RNAs. *Cell* **129**, 1311–1323 (2007).
20. Khalil, A.M. *et al.* Many human large intergenic noncoding RNAs associate with chromatin-modifying complexes and affect gene expression. *Proc. Natl. Acad. Sci. USA* **106**, 11667–11672 (2009).
21. Li, X. *et al.* A maternal-zygotic effect gene, *Zfp57*, maintains both maternal and paternal imprints. *Dev. Cell* **15**, 547–557 (2008).
22. Collins, R.E. *et al. In vitro* and *in vivo* analyses of a Phe/Tyr switch controlling product specificity of histone lysine methyltransferases. *J. Biol. Chem.* **280**, 5563–5570 (2005).
23. Nishikawa, S., Goldstein, R.A. & Nierras, C.R. The promise of human induced pluripotent stem cells for research and therapy. *Nat. Rev. Mol. Cell Biol.* **9**, 725–729 (2008).
24. Soldner, F. & Jaenisch, R. Medicine. iPSC disease modeling. *Science* **338**, 1155–1156 (2012).
25. Chamberlain, S.J. *et al.* Induced pluripotent stem cell models of the genomic imprinting disorders Angelman and Prader-Willi syndromes. *Proc. Natl. Acad. Sci. USA* **107**, 17668–17673 (2010).
26. Yang, J. *et al.* Induced pluripotent stem cells can be used to model the genomic imprinting disorder Prader-Willi syndrome. *J. Biol. Chem.* **285**, 40303–40311 (2010).
27. Cabili, M.N. *et al.* Integrative annotation of human large intergenic noncoding RNAs reveals global properties and specific subclasses. *Genes Dev.* **25**, 1915–1927 (2011).
28. Mann, M.R. & Bartolomei, M.S. Towards a molecular understanding of Prader-Willi and Angelman syndromes. *Hum. Mol. Genet.* **8**, 1867–1873 (1999).
29. Falk, M.J., Curtis, C.A., Bass, N.E., Zinn, A.B. & Schwartz, S. Maternal uniparental disomy chromosome 14: case report and literature review. *Pediatr. Neurol.* **32**, 116–120 (2005).
30. Hordijk, R. *et al.* Maternal uniparental disomy for chromosome 14 in a boy with a normal karyotype. *J. Med. Genet.* **36**, 782–785 (1999).
31. Hosoki, K. *et al.* Maternal uniparental disomy 14 syndrome demonstrates Prader-Willi syndrome–like phenotype. *J. Pediatr.* **155**, 900–903 (2009).
32. Reik, W. & Walter, J. Evolution of imprinting mechanisms: the battle of the sexes begins in the zygote. *Nat. Genet.* **27**, 255–256 (2001).

ONLINE METHODS

Cell culture. The PWS primary fibroblast cell line WG1534 (PWS-1) was purchased from the Repository for Mutant Human Cell Strains at McGill University Health Centre/Montreal Children's Hospital. The PWS primary fibroblast cell line GM21889 (PWS-2) was purchased from the Coriell Institute for Medical Research. Fibroblasts obtained from an individual with PWS harboring complete mUPD of chromosome 15 (PWS-3) were obtained with national (920110641) and institutional (SZMC-IRB 88/11) ethical approvals. Cells were cultured in MEM (Sigma, M5650) supplemented with 15% FCS, 2 mM L-glutamine, 50 units/ml penicillin and 50 μg/ml streptomycin. All PSC cultures were maintained on a feeder layer of mitomycin-arrested mouse embryonic fibroblasts (MEFs) and were grown in human ESC medium containing Knockout DMEM (Gibco) supplemented with 15% Knockout Serum Replacement (Gibco), 2 mM L-glutamine (Biological Industries), 0.1 mM nonessential amino acids (Biological Industries), 0.1 mM β-mercaptoethanol and 8 ng/ml basic fibroblast growth factor (bFGF; Cytolab). All cells were free of mycoplasma and were maintained in a humidified incubator at 37 °C and 5% CO_2. PSCs were collected using trypsin (Biological Industries). For embryoid body (EB) formation, cells were collected from a semiconfluent six-well plate of PWS-iPSCs using trypsin, and cell clumps were resuspended in ESC medium without bFGF, allowed to aggregate and transferred to one well of a six-well plate. After 20 d, EB RNA was isolated and analyzed. PWS B lymphocyte–derived cell lines (GM21891 and GM13553, Coriell Institute for Medical Research) were cultured on non-adherent plates and cultured in RPMI-1640 medium (Sigma) supplemented with 15% FBS, 50 units/ml penicillin and 50 μg/ml streptomycin.

Generation of PWS induced pluripotent stem cells. Reprogramming of PWS fibroblasts to pluripotency was established as described previously[7]. Briefly, for production of viral particles, 293T cells (obtained from R. Weinberg, Whitehead Institute) were transfected using TransIT-LT1 transfection reagent (Mirus) with 4.5 μg of pMXs retroviral vectors containing human *POU5F1* (*OCT4*), *SOX2*, *KLF4* or *MYC* and 4.5 μg of PCL-Ampho plasmid. Twenty-four hours after transfection, culture medium was replaced with fresh medium, and, 48 h after transfection, the supernatant was collected, filtered through a 0.45-μm cellulose acetate filter (Whatman) and supplemented with 4 μg/ml polybrene (Sigma-Aldrich). Fibroblasts (600,000 from each aces) were infected with viral particles encoding the four factors. On day 4 after infection, cells were transferred to ESC growth conditions, supported by mitomycin-arrested MEF feeders. Morphological changes began to occur around day 12. ESC-like colonies showed morphological resemblance to ESC colonies and were manually expanded.

Cerebrum brain samples. PWS and control cerebrum brain tissues were purchased from the National Institute of Child Health and Human Development (NICHD) Brain and Tissue Bank for Developmental Disorders, University of Maryland, School of Medicine. Brain samples from PWS cases 5441 (~1 year old, male, African American) and 5324 (18 years old, male, Caucasian) were analyzed with respect to proper age- and sex-matched control individuals 1671 (~1 year old, male, African American) and 1409 (18 years old, male, Caucasian).

Alkaline phosphatase staining and immunocytochemistry. Alkaline phosphatase staining was performed with the Leukocyte Alkaline Phosphatase kit (Sigma), according to the manufacturer's instructions. For immunocytochemistry staining, cells were fixed with PBS containing 4% paraformaldehyde for 10 min at room temperature. After washing with PBS, cells were blocked for 1 h with PBS containing 2% BSA (Sigma) and 0.1% Triton X-100. Staining with primary antibodies was performed for 1 h at room temperature with antibodies diluted in blocking buffer as follows: OCT4 (1:150 dilution; Santa Cruz Biotechnology, sc-9081) and TRA-1-60 (1:200 dilution; Santa Cruz Biotechnology, sc-21705). Secondary antibodies used were cyanine 3 (Cy3)-conjugated rabbit anti-mouse IgM or rabbit anti-mouse IgG (1:200 dilution; Jackson ImmunoResearch Laboratories) following staining with Hoechst 33342 to detect the cell nucleus (Invitrogen).

Isolation of genomic DNA and RNA and reverse transcription. Total genomic DNA was extracted using the Nucleic Acid and Protein Purification kit (Macherey-Nagel Corporation), and RNA (DNase treated) was purified with the PerfectPure RNA Cultured Cell kit (5 PRIME). Total RNA (1 μg) was used for reverse transcription using ImProm-II reverse transcriptase (Promega) with random hexamer primers. For *IPW*-specific reverse transcription, a single primer was used, corresponding to the gene's transcription start site (20 μM). For sequencing and quantitative experiments, PCR was performed with GoTaq (Promega), whereas, for cloning of *IPW*, Platinum Pfx DNA Polymerase (Invitrogen) was used. qRT-PCR was performed with 1 μg of RNA reverse transcribed to cDNA and TaqMan Universal Master Mix or SYBR Green qPCR Supermix. Data were analyzed with the 7300 RT-PCR system (Applied Biosystems). A full description of primer sequences and annealing temperature can be found in **Supplementary Table 3**.

DNA microarray analysis. Total RNA was extracted according to the manufacturer's protocol (Affymetrix). RNA was subjected to the Human Gene 1.0 ST microarray platform (Affymetrix). Washing, and scanning were performed according to the manufacturer's protocol. Arrays were analyzed using Robust Multichip Analysis (RMA) in the Affymetrix Expression Console. Microarray data were deposited at GEO under accession GSE56136.

miRNA expression analysis. Total RNA was extracted using the MirVana miRNA isolation kit (Ambion). RNA was subjected to the Human GeneChip miRNA array platform (Affymetrix), according to the manufacturer's protocol. Data were normalized using the miRNA QC Tool (Affymetrix).

RNA sequencing analysis. High-throughput RNA sequencing analysis was performed as previously described[10].

Pyrosequencing analysis. Pyrosequencing was performed by EpigenDx using the PSQ96HS system according to standard procedures with a unique set of primers for CpG sites of the IG-DMR (ADS2273) at chr. 14: 101,277,218–101,277,286 (GRCh37/hg19 genome assembly).

Knockdown of *RTL1* in normal PSCs. For siRNA transfection, normal PSCs were dissociated using TrypLE Select (Gibco), resuspended in human ESC medium and transected with 5 μl of 20 μM ON-Target-Plus smart pool siRNA (Thermo Scientific) using Lipofectamine 2000 reagent (Life Technologies) according to the manufacturer's instructions. Cells were collected for RNA extraction 72 h after transfection.

Manipulation of *IPW* in Pg-iPSCs and PWS-iPSCs. For overexpression experiments, *IPW* transcript sequence was amplified by PCR (see full primer list in **Supplementary Table 3**) and cloned into an N1-EGFP vector using the DNA Ligation kit (Mighty Mix, TaKaRa). Electroporation was used (Gene Pulser Xcell, Bio-Rad; 320 V, 200 μF, 4-mm cuvette) to transfect both Pg-iPSCs and PWS-iPSCs. In each case, 20 μg of plasmid DNA was used. For control, cells were transfected with either a *HOTAIR* overexpression vector[33] or with empty N1-EGFP vector, using the same conditions.

Chromatin immunoprecipitation. Cells were cross-linked with 1% formaldehyde, resuspended in 150 μl of SDS lysis buffer on ice for 10 min and then sonicated using a Bioruptor bath sonicator (Diagenode) to an average DNA size of 750 bp. Chromatin was precleared with 40 μl of salmon sperm DNA–protein A–agarose beads (Upstate Biotechnology) for 1 h, followed by an overnight incubation with 5–10 μg of antibody to either H3K9me3 or H3K27me3 (Millipore, 07-442 and 07-449, respectively). As a control, samples were immunoprecipitated with non-immune rabbit IgG (Rockland). Chromatin-antibody complexes were eluted from protein A–agarose beads by the addition of 500 μl of elution buffer (1% SDS, 0.1 M $NaHCO_3$). Cross-linking was reversed by incubation of the eluted samples for 4 h at 65 °C under high-salt conditions. Proteins were digested using proteinase K treatment for 1 h at 45 °C. DNA was extracted with phenol-chloroform, precipitated with ethanol and dissolved in TE buffer.

doi:10.1038/ng.2968

RNA immunoprecipitation. RIP experiments were conducted as described at http://www.abcam.com/epigenetics/rna-immunoprecipitation-rip-protocol in a normal ESC line (H9) with antibodies against SUV39H1 (Santa Cruz Biotechnology, sc-377112; 10 µg) and G9A (R&D, PP-A8620A-00; 5 µg)[34].

33. Gupta, R.A. *et al.* Long non-coding RNA *HOTAIR* reprograms chromatin state to promote cancer metastasis. *Nature* **464**, 1071–1076 (2010).
34. Epsztejn-Litman, S. *et al. De novo* DNA methylation promoted by G9a prevents reprogramming of embryonically silenced genes. *Nat. Struct. Mol. Biol.* **15**, 1176–1183 (2008).